On the Feasibility of Overcoming Frequency Encoding Limitations Near Metal Implants with Broadband Single-Point Imaging on Clinical MR Systems

Kevin Koch[1] and Graeme McKinnon[1]
[1]*GE Healthcare, Milwaukee, WI, United States*

Target Audience: This work is target towards clinicians attempting to visualize tissue and bone in the presence of metallic hardware and physicists seeking solutions to further reduce residual artifacts near such implants

Purpose: Metal artifact reduction sequences, such as 3D-MSI, can substantially reduce bulk distortions near metallic hardware. However, it has recently been shown that such sequences are vulnerable to limitations inherent to any frequency-encoded acquisitions. These limitations generate residual signal loss in high local field-gradient regions near some implants, such as metal-on-metal hip replacements at 3T. Here we investigate a means whereby such signal loss can be regained using single-point-imaging (SPI) approaches on a clinical MR imaging system.

Methods: A clinically viable constant-time SPI approach was analyzed in this work. The major advantages of such an approach are a) zero distortions from spatial encoding and b) ultra-broadband excitation. Our implant-based models predict maximum spectral coverage ranges of roughly 75-80kHz for some commonly encountered orthopedic implants at 3T. The approach analyzed here assumes a SPRITE-like acquisition [1], whereby gradients are played out during RF and the phase-encode occurs between the RF perturbation and acquisition. This encode time, T_P, is dependent on systematic limitations (e.g. receiver unblanking). Simulations were constructed assuming hardware limitations on an existing clinical MR system (Discovery MR750w, GE Healthcare) that has already demonstrated and established a capability for ZTE technology. On this system, hardware limitations set a minimum T_p at roughly 50us. The maximum resolution for a constant time SPI approach is then determined by the maximum imaging gradient strength, which is 30 mT/m on the target hardware. Under such constraints, the maximum resolution for a 50us T_p time is roughly 4mm. The acquisition time for such clinically viable SPI sequences can also be estimated from the minimum TR on the target hardware -- which is roughly 200us beyond the acquisition point (T_p).

Here we examine if such a clinically viable SPI acquisition may be useful to detect residual signal that is unobtainable with 3D-MSI sequences. The key point of analysis is T2* signal loss that will be found in the high-gradient regions that cause signal dropout in the frequency-encoded images.

A computational artifact prediction method from a metal-on-metal total hip implant model was utilized to study this effect. The B_0 perturbation induced by the implant at 3T was estimated from a forward perturbation field prediction model [2]. Conventional (frequency-encoded) imaging artifacts were estimated from local induction gradients in the frequency-encoded dimension (S/I, top-down). As shown in [3], signal loss was predicted in areas where the local gradient surpassed the magnitude of the applied frequency-encoding gradient (500 Hz/px). T2* loss was estimated in the SPI sequences by assuming sinc() signal loss model as a function of the local through-voxel gradient in all 3 dimensions [4].

Metal-on-Metal Total Hip at 3T

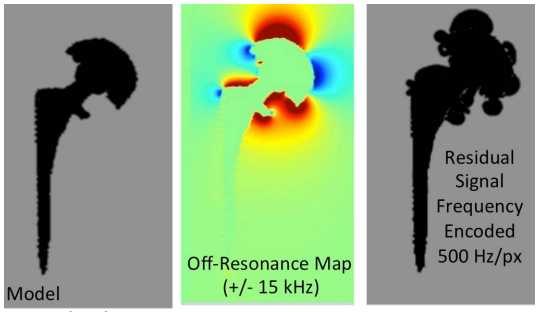

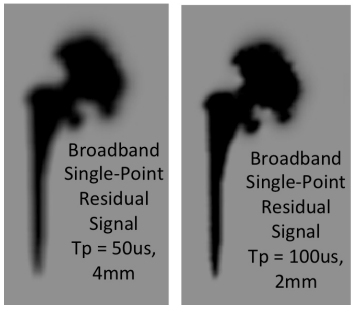

Results: The utilized metal-on-metal model and off-resonance distribution are displayed. Using these models, the residual signal in a 3D-MSI sequence using a 500 Hz/px frequency-encoding gradient is shown. 3D-MSI sequences do not suffer from bulk distortions, so these signal artifacts are the primary residual artifacts in a 3D-MSI sequence. Two SPI implementations are then shown, using 4 mm resolution with Tp = 50us and 2mm (in-plane) resolution using T_p = 100us. It is clear that there is some remaining signal loss in the SPI implementations. However, it is also clear that a great deal of the missing signal in the frequency-encoded acquisition can be regained with broadband SPI. Note that there is not a substantial loss in spatial signal extent between these two SPI settings. This because the extra T2* dephasing evolution is largely compensated by the reduced voxel extent. A similar simulation was performed on a metal-on-poly implant with a plastic liner in the hip socket. Clinicians could benefit from the signal available in such plastic components, which could be visible with SPI encode times [1]. The lower right image shows the results of this simulation, and demonstrates that some, but not all of the liner may be visible. This hints at likely difficulties (at 3T) in using SPI to detect plastic components near implant surfaces.

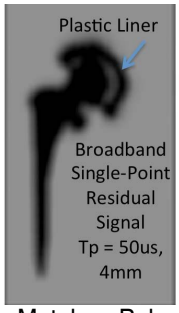

Metal-on-Poly

Discussion: It is clear from these results that there is signal to be gained from clinical application of SPI methods to imaging near metal implants at 3T. Such acquisitions could be used to fuse-with or supplement existing 3D-MSI approaches. The scan times for the presented high-bandwidth SPI acquisitions can be estimated as follows. Consider a typical 3D-MSI hip image of 40cm coronal field-of-view with 24 4mm slice-encodes. The 4mm SPI acquisition then requires a 100x100x24 acquisition grid. Using the 250us TR limitation, this yields only a 60 second scan time. The 2mm (in-plane) SPI acquisition (200x200x24, TR = 300us) would then require roughly 5.5 minutes. Barring an SNR analysis of such acquisitions, there is likely room to reduce these scan times even further through parallel imaging. More resolution may also be achievable, but will be largely a function of applied undersampling schemes and available SNR.

Conclusion: A model has been presented to estimate the viability of broadband SPI methods in acquiring residual signal that is not attainable with existing 3D-MSI artifact reduction sequences. Such images have limitations due to hardware constraints. However, there may still be useful information contained in these images to improve assessment of tissue and bone pathology near metallic hardware. Further work will implement the simulated methods and compare the observed images with these computed results, as well as compare the trade-offs of this approach with alternate demonstrations of single point imaging near metal [5].

[1] Ramos-Cabrer, MRI, 22, 1097-1103, 2004, [2] Koch et al, Proc ISMRM, 1180, 2008, [3] Koch et al, MRM, 2013, doi: 10.1002/mrm
[4] Zhao et al, JMR. 173, 10–22, 2005 , [5] Artz et al, MRM, 2013, doi: 10.1002/mrm.24704